Structure of $(AgI)_x$-$(Ag_2O$-$nB_2O_3)_1$-x glasses by neutron diffraction and reverse Monte Carlo simulations

1999 J. Phys.: Condens. Matter 11 9275

(http://iopscience.iop.org/0953-8984/11/47/312)

J. Phys.: Condens. Matter **11** (1999) 9275–9291. Printed in the UK PII: S0953-8984(99)06781-8

Structure of $(AgI)_x$–$(Ag_2O$–$nB_2O_3)_{1-x}$ glasses by neutron diffraction and reverse Monte Carlo simulations

J Swenson†, L. Börjesson† and W S Howells‡

† Department of Applied Physics, Chalmers University of Technology, S-412 96 Göteborg, Sweden

‡ Rutherford–Appleton Laboratory, Chilton, Didcot OX11 0QX, UK

Received 9 August 1999

Abstract. The structures of the ion conducting glasses Ag_2O–$4B_2O_3$, AgI–Ag_2O–$4B_2O_3$ and $(AgI)_{0.6}$–$(Ag_2O$–$B_2O_3)_{0.4}$ have been investigated by neutron diffraction experiments and reverse Monte Carlo (RMC) modelling. The results are compared with previous findings for the diborate glass system $(AgI)_x$–$(Ag_2O$–$2B_2O_3)_{1-x}$. The experimental pair correlation functions support previous NMR results and indicate that the fraction of four-coordinated boron atoms is considerably higher in the metaborate glass than in the two tetraborate glasses and also slightly higher than for the diborate glasses. The intermediate range order within the B–O network of the AgI doped tetra- and metaborate glasses is less pronounced than for the correspondingly doped diborate glasses. The structures of the tetraborate glasses can be considered to be a microscopic mixture of the correspondingly doped diborate glasses and pure B_2O_3, containing two distinct characteristic intermediate range distances within the B–O network. The $(AgI)_{0.6}$–$(Ag_2O$–$B_2O_3)_{0.4}$ glass shows an extraordinary intense prepeak at an anomalously low Q-value of 0.46 Å^{-1} in the total neutron structure factor. However, despite its intensity the RMC produced structural model indicates that the peak is not due to any specific well defined correlation on a corresponding length scale. Rather, the prepeak seems to arise from a combination of partial structure factors with increasing and decreasing intensities in the actual Q-range, although the high intensity of the peak is mainly due to large density fluctuations within the B–O network. Some small (∼10 Å) clusters of AgI are observed in the large voids of the B–O structure. Furthermore, the RMC produced model of the AgI doped metaborate glass had a higher average Ag–Ag coordination number than previously has been observed for other highly conducting oxide based glasses. The high Ag–Ag coordination may give rise to a strong cationic Coulomb interaction and result in a non-Arrhenius temperature behaviour of the conductivity, as recently has been suggested by Maass *et al* (1996 *Phys. Rev. Lett.* **77** 1528).

1. Introduction

Fast ion conducting solids show the remarkable behaviour of a selective ion mobility in an otherwise frozen glass matrix. The glassy conductors are of interest for technological applications, e.g. as solid electrolyte in electrochemical devices such as batteries, sensors, 'smart windows' etc. Particular advantages of glassy ion conductors are their ease of preparation, their stability and the large available composition ranges. In order to understand the diffusion mechanism and be able to improve the conductivity it is important to obtain more insight into the relation between microscopic structure and ionic conductivity.

Recently there have been new experimental indications that the highest obtainable ionic conductivity at room temperature is in the range 10^{-2}–10^{-1} S cm^{-1} for glassy electrolytes [1]. By using all the known empirical rules of thumb for high ionic conductivity, i.e. using

0953-8984/99/479275+17$30.00

a relatively small and highly polarizable cation, a large and also polarizable anion, a mixture of glass-formers and sulphide-based glasses, Kincs and Martin [1] developed the new glass system $(AgI)_x$–$[0.525Ag_2S$–$0.475(0.5B_2S_3$–$0.5SiS_2)]_{1-x}$ with a record high sub-ambient temperature conductivity of several orders of magnitude higher than has previously been observed for traditional oxide-based glassy electrolytes (e.g. AgI doped silver phosphate, borate and molybdate glasses) [2]. However, due to the fact that the silver thio-boro-silicates exhibited a strong non-Arrhenius behaviour even far below room temperature the difference in conductivity vanished at room temperature, where both the thio-boro-silicate glasses and the oxide-based phosphate, borate and molybdate glasses show conductivity values of about 10^{-2} S cm^{-1}. The deviation from Arrhenius behaviour increased with increasing AgI content which contributed to the fact that the introduced salt ions had only a small effect (less than one order of magnitude) on the conductivity at room temperature. Similar non-Arrhenius behaviours have been observed also for the highest conducting oxide glasses [3], α-AgI-frozen composites of $(AgI)_x$–$(3Ag_2O$–$B_2O_3)_{1-x}$ ($x > 0.6$) [4] and crystalline conductors [5] when the conductivity approaches 10^{-3} S cm^{-1}. Thus, this seems to be an universal behaviour pointing towards a fundamental limitation of the ionic conductivity in solid electrolytes.

Some explanations for the non-Arrhenius behaviour and the related 'saturation effect' have recently been put forward. It has been proposed that there is a 'mobile ion glass transition' and that the conductivity simply follows the common empirical Vogel–Fulcher–Taummann (VFT) law above this glass transition (rather than above the normal glass transition, which is the behaviour for less conducting glasses) [5]. The 'mobile ion glass transition' is given by T_0 in the VFT law and it is assumed to be the lowest temperature where the cations are able to distribute themselves among the equivalent energetically available positions. Another explanation for the non-Arrhenius behaviour is that the activation energy for ionic diffusion is determined by the sum of two contributions, where the first term is due to the energy difference between different sites and the second term is related to Coulomb interaction between the mobile ions [9]. The first term is thus related to the disorder in the structure and it reduces when the temperature is raised and finally at relatively high temperatures the Coulombic term becomes dominant. Thus, the cross-over temperature from Arrhenius to non-Arrhenius behaviour is given by the cross-over between the two temperature regimes of the activation energy. The non-Arrhenius behaviour is also explained within the coupling model [10], where the experimentally observed cross-over from a high activation energy at low temperatures to a lower activation energy at high temperatures is reproduced by the introduction of a microscopic time t_c. Before t_c interactions between ions have no effect on the dynamics of an ion and at longer times interactions between the ions set in and reduce the conductivity.

The AgI doped silver borate glass system $(AgI)_x$–$(Ag_2O$–$nB_2O_3)_{1-x}$ shows an analogous behaviour to the thio-boro-silicate glasses both in the sense of the non-Arrhenius behaviour for the highest network modified and salt doped compositions and in the sense that there seems to be an upper limit for the conductivity. The difference in conductivity between the meta- and tetraborate systems is, for example, reduced from five orders of magnitude at the dopant concentration $x = 0.2$ to only one order of magnitude at $x = 0.6$ [6]. The aim of this investigation is to understand this on a structural basis and to elucidate whether the intermediate range order or local environment of the silver ions changes more rapidly with the dopant concentration for the tetraborate composition than for the correspondingly doped di- and metaborate glasses. Furthermore, we aim to find a possible structural explanation for the 'saturation effect' of the conductivity, which seems to exist for all highly conducting glasses.

Previous studies of AgI doped diborate, metaphosphate and molybdate glasses have indicated two important facts: first, that the increase in conductivity with increasing dopant concentration is closely related to the salt induced expansion of the glass matrix [7] and,

second, that the local average environment of the Ag^+ ions is similar for glasses with similar conductivity [8]. These empirical observations seem to be rather general and are likely to hold for most metal-halide doped oxide glasses [7]. However, from the present investigation there seems to be smaller deviation from this behaviour for the highly doped metaborate glasses. The $(AgI)_x$–$(Ag_2O–B_2O_3)_{1-x}$ system is glass forming up to $x = 0.8$, which with the empirical conductivity versus network expansion relation would predict a slightly higher conductivity (of the order of 0.1 S cm^{-1} rather than the observed 0.03 S cm^{-1} [2]) and, as the present study will show, a higher conductivity would also be expected from the observed local average environment of the Ag^+ ions. Thus, it appears that there is a cross-over from the empirical structure–conductivity relations and the normal Arrhenius law at a certain ratio between the thermal energy and the activation energy for ion conduction, where other structural or dynamical properties of the solid electrolytes begin to have a detrimental effect on the conductivity.

2. Experimental procedure

2.1. Sample preparation

The $Ag_2O–4B_2O_3$, $AgI–Ag_2O–4B_2O_3$ and $(AgI)_{0.6}$–$(Ag_2O–B_2O_3)_{0.4}$ glasses were prepared using a conventional melt quenching method according to procedures described previously [11, 12]. In all samples boron was isotopically enriched in ^{11}B (99%) in order to minimize the influence of the high neutron absorption of ^{10}B present in natural boron. The samples were in shapes of cylindrical rods with a diameter of 9 mm and a length of 50 mm. The mass density of the samples was measured by the Archimedes method using methanol. The atomic number densities were 0.0834, 0.0775 and 0.059 Å^{-3} (with error bars of ±2%) for the $Ag_2O–4B_2O_3$, $AgI–Ag_2O–4B_2O_3$ and $(AgI)_{0.6}$–$(Ag_2O–B_2O_3)_{0.4}$ glasses.

2.2. Neutron diffraction

The samples for the neutron diffraction experiments were placed in thin walled vanadium containers. The experiments were performed on the time-of-flight Liquid and Amorphous Materials Diffractometer (LAD) at the pulsed neutron source ISIS, Rutherford–Appleton Laboratory, UK. The diffractometer has been described in detail elsewhere [13]. Time-of-flight spectra were recorded separately for each group of detectors at the angles 150, 90, 58, 35, 20, 10 and 5° and also for monitors in the incident and transmitted beam, respectively. The data of each detector group were corrected separately for background and container scattering, absorption, multiple scattering and inelasticity effects, and normalized against the scattering of a vanadium rod to obtain the structure factor, $S(Q)$, following the procedure described in [14]. The corrected individual data sets obtained at each angle were then combined to obtain a wide Q-range and to improve the statistics. For each data set we only used the Q-range that agreed with other data sets in the overlapping Q-region.

The obtained structure factor, $S(Q)$, of each sample was truncated at $Q_{max} = 30$ Å^{-1} in order to avoid small systematic errors of the high-Q data and then Fourier transformed to obtain the total neutron weighted pair correlation function

$$G(r) = \left(\sum_{i=1}^{n} c_i b_1^2\right)\left[2\pi^2\rho^0\left(\sum_{i=1}^{N} c_i b_i\right)^2\right]^{-1}\int_0^\infty Q(S(Q)-1)\sin(Qr)\,\mathrm{d}Q + 1 \qquad (1)$$

where ρ^0 is the average number density, and c_i and b_i are the concentration and neutron scattering length of atom i, respectively. Termination ripples in the correlation function

caused by the truncation and Fourier transformation of $S(Q)$ were reduced by multiplying the integrand in equation (1) with a Lorch modification function [15], although this is at the expense of a somewhat reduced real space resolution.

The total $G(r)$ can be expressed as a neutron weighted (i.e. dependent upon the scattering lengths of the constituent atoms) sum of the partial pair correlation functions $g_{ij}(r)$ according to

$$G(r) = \left(\sum_{i,j=1}^{n} c_i c_j \langle b_i \rangle \langle b_j \rangle g_{ij}(r) \right) \left[\left(\sum_{i=1}^{N} c_i b_i \right)^2 \right]^{-1}. \tag{2}$$

3. Experimental results

The total neutron structure factors, $S(Q)$, for Ag_2O–$4B_2O_3$, AgI–Ag_2O–$4B_2O_3$ and $(AgI)_{0.6}$ –$(Ag_2O$–$B_2O_3)_{0.4}$ are shown in figure 1. From the figure it is evident that the two tetraborate glasses show almost identical results for the high Q-range, indicating that the dopant ions enter interstices and voids of the host B–O network structure without affecting its short range order. However, in the low Q-region below 5 Å^{-1} there are clear differences between the investigated glasses. The undoped tetraborate glass shows a relatively strong peak located at 1.85 Å^{-1} and a weak peak and a shoulder at 3.15 and 1.35 Å^{-1}, respectively. The intensity of the shoulder at 1.35 Å^{-1} increases with increasing Ag_2O modification and is observed as a well resolved sharp diffraction peak (FSDP) for the diborate glass [16]. In the case of the AgI doped tetraborate glass the positions of the main peak and the small peak have shifted to slightly lower Q-values (1.70 and 3.05 Å^{-1}) and increased in intensity. The most interesting feature is, however, that the doped glass shows a new prepeak located at 0.79 Å^{-1} (i.e. at the same position, but with lower intensity than for the corresponding diborate composition AgI–Ag_2O–$2B_2O_3$ [17]). Turning to the AgI doped metaborate glass, the $S(Q)$ is completely different in the low Q-range and also slightly different at higher Q-values, indicating both a new kind of intermediate range ordering as well as slightly different short range structural units. The most remarkable feature of $S(Q)$

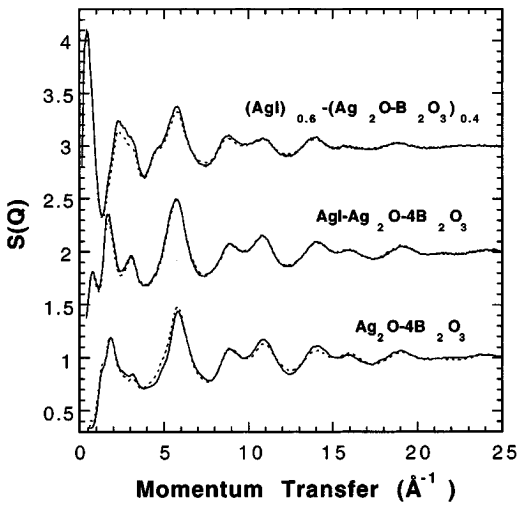

Figure 1. Experimental structure factors $S(Q)$ (full lines) and computed neutron weighted total structure factors (dashed lines) for the RMC produced configurations of (a) Ag_2O–$4B_2O_3$, (b) AgI–Ag_2O–$4B_2O_3$ and (c) $(AgI)_{0.6}$–$(Ag_2O$–$B_2O_3)_{0.4}$. The upper curves have been shifted vertically by 1.0, for clarity.

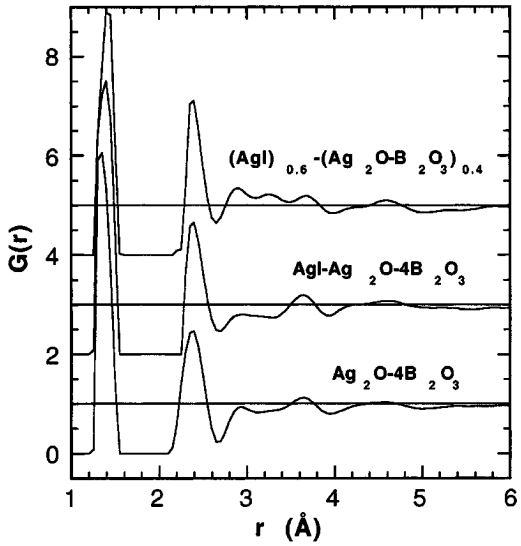

Figure 2. Experimental pair correlation functions, $G(r)$, for the same glasses as shown in figure 1. Consecutive curves are shifted vertically by 2.0, for clarity.

for the AgI doped metaborate glass is the extraordinary intense FSDP at the anomalously low Q-value 0.46 Å^{-1}, corresponding to a real space characteristic distance of the order of $2\pi/Q \sim 14$ Å.

To investigate the details of the short range correlations, the $S(Q)$ shown in figure 1 have been Fourier transformed to the corresponding atomic pair correlation functions, $G(r)$, in figure 2. The figure confirms that the short range order (the nearest B–O distance at about 1.4 Å and the B–B and O–O peak at about 2.4 Å) of the B–O network is similar for the three glasses. The most significant difference is that the first B–O distance is considerably larger for the $(AgI)_{0.6}$–$(Ag_2O$–$B_2O_3)_{0.4}$ glass (about 1.42 Å) than for the salt doped tetraborate glass (1.38 Å), indicating a higher fraction of four coordinated borons in the metaborate glass [16]. This is also confirmed from an integration over the first B–O peak, which gives the B–O coordination numbers 3.14, 3.21 and 3.45 for the Ag_2O–$4B_2O_3$, AgI–Ag_2O–$4B_2O_3$ and $(AgI)_{0.6}$–$(Ag_2O$–$B_2O_3)_{0.4}$ glasses, respectively. In the slightly higher r-range the most pronounced difference between the three $G(r)$-functions is observed in the range $2.8 < r < 3.4$ Å, where the salt doped metaborate glass shows significantly higher intensity, most likely due to the nearest Ag–I and Ag–Ag distances, as observed for AgI doped diborate glasses [17].

4. Reverse Monte Carlo modelling

4.1. The method

The RMC method [18, 19] has been extensively described elsewhere [20, 21] so here we will only give a brief summary and some details of the particular bonding constraints we have used in the simulations. RMC uses a standard Metropolis Monte Carlo algorithm [22], but, instead of minimizing the energy, one minimizes the squared difference between the experimental structure factor and the structure factor calculated from the computer configuration. Furthermore, the random atomic moves are only accepted if they are in

accordance with certain constraints, e.g. closest allowed atom–atom distances (see below). In this way, the RMC method produces three-dimensional models of disordered materials that agree quantitatively with the available diffraction data (provided that the data do not contain significant systematic errors) and the physical constraints applied.

4.2. Simulation procedure

To be able to model the intermediate range structural order and the thermal fluctuations of the glasses the configurations have to be large enough so that the corresponding box sizes do not influence the ordering and it is possible to approximate the thermal average by a single volume average. In the present case, the computer configurations of the two tetraborate glasses contained approximately 4000 atoms, whereas the metaborate glass contained as many as 32 000 atoms in order to be able to produce a structural model that accounts for the low Q-value of the FSDP. The configurations should then be large enough for modelling the intermediate range ordering observed in the present diffraction data. The box lengths were given values (approximately 40 Å for the tetraborate glasses and 80 Å in the case of the metaborate glass) corresponding to the experimentally measured densities. Periodic boundary conditions were used in cubic boxes.

In order to ensure physically realistic configurations it is important to include certain constraints in the simulations, such as minimum atomic sizes and density, as mentioned above. Furthermore, one has to use specific bonding constraints to ensure that the B and O atoms form a proper network. The closest distances that two atoms were allowed to approach were determined from the experimental results, e.g. the radial distribution functions, and tabulated ionic radii. The following closest atom–atom distances were used in the simulations: 1.25 Å for B–O, 2.0 Å for O–O, 2.1 Å for B–B and Ag–O, 2.5 Å for Ag–I, 2.6 Å for Ag–B, 2.7 Å for Ag–Ag, 2.8 Å for O–I, 3.2 Å for B–I and 3.6 Å for I–I. The constraints on the B–O network connectivity were applied on the basis of results obtained from magic angle spinning NMR [23, 24], Raman [25, 26] and infrared experiments [27], which have shown that the addition of M_2O to B_2O_3 causes a progressive increase in the number of four-coordinated borons at the expense of three-coordinated ones (up to 40–50% M_2O concentration). At the composition Ag_2O–$4B_2O_3$ the fraction of four-coordinated borons is close to 25%. Therefore, for the two tetraborate glasses we have applied the constraints that all the oxygens are coordinated (in the interval 1.25–1.65 Å) to two borons and that 25% of the borons are coordinated to four oxygens. The remaining borons are coordinated to three oxygens. This gives a 3D network of interconnected BO_3 and BO_4 units with no non-bridging oxygens. For the metaborate composition the B–O network is slightly more complicated and it seems as if the fraction of BO_4 units is cation dependent. The magic angle spinning NMR data [23] on Ag_2O–B_2O_3 show that the fraction of BO_4 units is approximately 53% and more detailed studies on lithium borate glasses have indicated that the remaining borons are located in metaborate structural groups [24], which must be the case also for Ag_2O–B_2O_3, provided that no loose BO_3 units are present. These metaborate groups consist of interconnected BO_3 triangles with one non-bridging oxygen per BO_3. Thus, the metaborate groups form chains of BO_3 triangles, where 50% of the oxygens are coordinated to two borons and the remaining 50% are coordinated to only one boron atom. If the appropriate fractions of BO_4 units and metaborate groups are added together we obtain the following constraints used in the RMC modelling of the metaborate glass: 53% of the borons were four coordinated to oxygens whereas the remaining borons were three coordinated. 76.5% of the oxygens were bridging between two borons and the remaining 23.5% of the oxygens were non-bridging and coordinated to only one boron. In this context one should note that the exact fractions of the different short range structural

units are not crucial for the conclusion of this paper, which mainly concerns the intermediate range order, as long as they are reasonable. After the B–O network was produced by a hard sphere Monte Carlo (HSMC) simulation all the Ag^+ and I^- ions were randomly added to the computer boxes. The salt ions were then moved apart from each other and from the B and O atoms in order to fulfil the closest atom–atom constraints.

In addition to the closest allowed atom–atom distances and connectivity constraints within the B–O network we have used a third kind of constraint during the RMC modelling. It is based on bond valence sums calculated from pseudopotentials and it is appropriate to use for interatomic correlations involving ions. The valence sum

$$V = \sum_X S_{Ag-X} \tag{3}$$

for each Ag^+ ion is calculated from empirical bond-length bond-valence equations. We have chosen the parameter set by Radaev *et al* [28, 29] given in equation (4).

$$S_{Ag-O} = \exp\left[\frac{1.89\ \text{Å} - R_{Ag-O}}{0.33\ \text{Å}}\right] \tag{4}$$

$$S_{Ag-I} = \exp\left[\frac{2.08\ \text{Å} - R_{Ag-I}}{0.53\ \text{Å}}\right]. \tag{5}$$

The authors obtained the parameter values by calculating the Ag^+ valence sums for different crystal structures and fitting the average values to 1, which is the expected valence sum for a monovalent cation such as Ag^+. All oxygens and iodine ions up to a distance of 6 Å ($R_{Ag-X} < 6$ Å) from the respective Ag site are included. For a physically correct structure with the atoms (or ions) in their local equilibrium positions it is expected that the valence sum V should be relatively close to a target valence of 1. Thus, we have used a constraint which minimizes the valence difference $\Delta V = |V - 1|$ for each Ag^+ ion. This should improve the correctness of the Ag coordinations, particularly in the present case where x-ray data, which are more sensitive to Ag correlations, are lacking. However, one should note that it has not been possible to fit the diffraction data with a strict constraint on the valence sum, indicating that the real valence sum of some of the individual Ag^+ ions deviates from the empirically expected value of 1 (at least partly due to the fact that the neutron data provide an instantaneous picture of the structure, where the atoms and ions are not necessarily located at their equilibrium positions).

4.3. Results

The neutron weighted structure factors of Ag_2O–$4B_2O_3$, AgI–Ag_2O–$4B_2O_3$ and $(AgI)_{0.6}$–$(Ag_2O$–$B_2O_3)_{0.4}$ obtained by RMC modelling are compared with those obtained experimentally in figure 1. The structure factors of the salt doped glasses are well reproduced over the whole Q-range, whereas the undoped tetraborate glass shows some smaller deviations from the experimental data, particularly in the Q-range 10–15 Å^{-1}. The deviations are probably mainly caused by systematic experimental or correction errors of the experimental data and perhaps some difficulties in the simulation to reproduce the complicated topology of the B–O network. One should however note that the FSDP, related to the intermediate range ordering, is well fitted for all glasses. Since the present analysis focuses on the intermediate range order and coordination of the cations, which has to be physically sensible due to the applied bond valence constraint, the relatively small differences between the experimental and RMC produced data should not have any major influence on the current study.

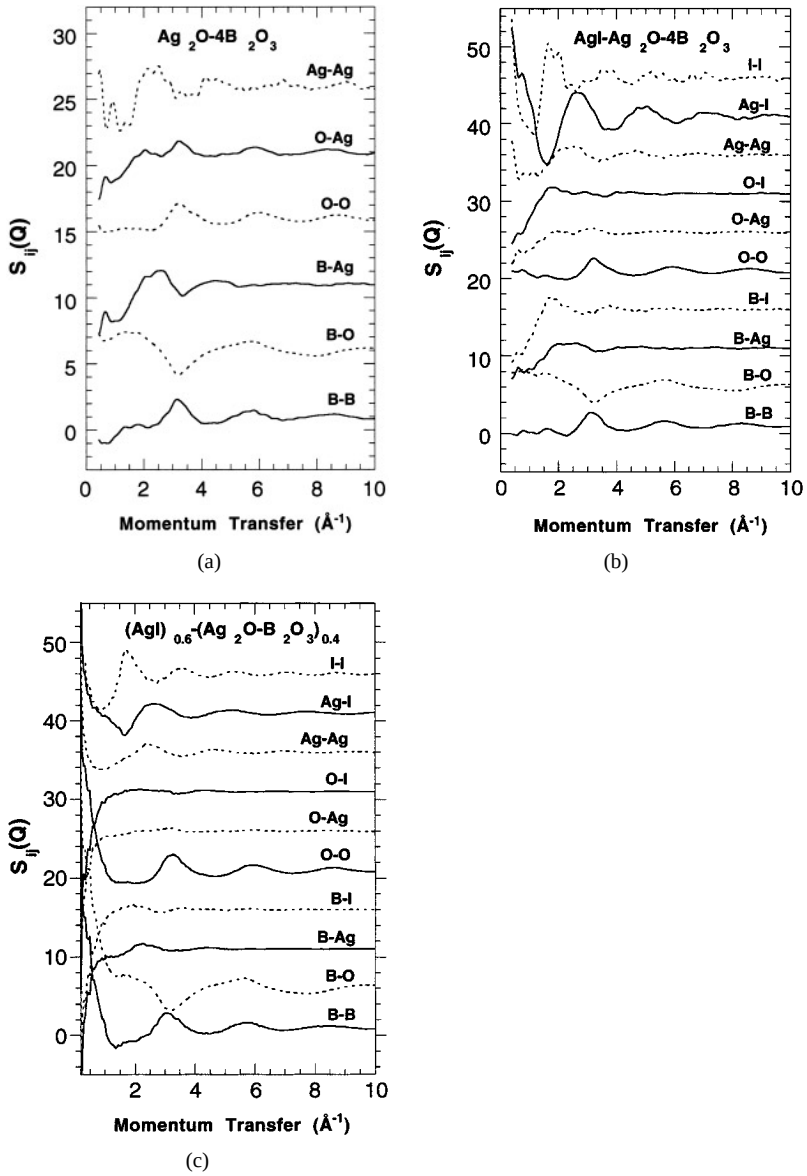

Figure 3. Partial structure factors, $S_{ij}(Q)$, calculated from the RMC produced configurations of (a) Ag_2O–$4B_2O_3$, (b) AgI–Ag_2O–$4B_2O_3$ and (c) $(AgI)_{0.6}$–$(Ag_2O$–$B_2O_3)_{0.4}$. Consecutive curves are shifted vertically by 5.0, for clarity.

4.3.1. Intermediate range order. In figures 3(a)–(c) we plot the partial structure factors $S_{ij}(Q)$ for the RMC produced configurations of Ag_2O–$4B_2O_3$, AgI–Ag_2O–$4B_2O_3$ and $(AgI)_{0.6}$–$(Ag_2O$–$B_2O_3)_{0.4}$, respectively. Figure 3(a) shows that for Ag_2O–$4B_2O_3$ the FDSP at 1.85 Å^{-1} in the total $S(Q)$ is mainly due to relatively weak B–O and B–B correlations. The FSDP, and thus also the intermediate range order, of the B–O network of Ag_2O–$4B_2O_3$ is, in fact, less pronounced than for both pure B_2O_3 [30] and Ag_2O–$2B_2O_3$ [17], where the $S_{BB}(Q)$-, $S_{BO}(Q)$- and $S_{OO}(Q)$-partials show evidence of a typical characteristic distance within the

B–O network. In the case of the RMC model of the diborate composition the three partials involving correlations within the B–O network showed peaks at about 1.2 $Å^{-1}$, and were interpreted as arising from a characteristic correlation between neighbouring borate segments separated by bridging Ag^+ ions to a distance of approximately 5 Å [17]. Such a correlation (although much less pronounced) is clearly present also in the tetraborate glass, and is indicated by the weak peaks or shoulders in $S_{BB}(Q)$, $S_{BO}(Q)$ and $S_{OO}(Q)$ at about the same Q-value (note also the shoulder at 1.35 $Å^{-1}$ in total $S(Q)$). The shorter correlations within the B–O network giving rise to the FSDP at 1.85 $Å^{-1}$ originate probably from correlations between segments or regions of the network where no Ag^+ ions are present in the absolute vicinity.

For the AgI doped tetraborate glass it is seen in figure 3(b) that the two first diffraction peaks located at 0.79 and 1.7 $Å^{-1}$ in the total $S(Q)$ are visible in all the three $S_{ij}(Q)$ involving correlations within the B–O network. Thus, two distinctly different correlation lengths of about 8 and 4 Å ($\sim 2\pi/Q$) are observed within the B–O network. The longer correlation length is the same as has been observed for AgI doped diborate glasses [17] and is interpreted as a characteristic distance between neighbouring borate segments separated by Ag–I–Ag bridges (in a simplified picture) in the network structure. This interpretation of the first peak for the AgI doped tetraborate glass is supported by the corresponding x-ray data, which are weighted strongly to correlations involving Ag^+ and I^- ions and shows a less intense FSDP at about 0.9 $Å^{-1}$ [31]. Thus, the FSDP at 0.79 $Å^{-1}$ in the neutron data, which is weighted predominantly to B and O correlations, is mainly due to correlations between the light B and O atoms. The shorter distance is, as for the undoped glass, probably a typical distance within the B–O network where no Ag^+ or I^- ions are present in the absolute vicinity, since the corresponding Q-value of the peak (1.7 $Å^{-1}$) is more similar to the position of the FSDP at 1.6 $Å^{-1}$ for pure B_2O_3 [30].

As already mentioned, magic angle spinning NMR data [23, 24] on silver and lithium metaborate glasses showed that the B–O network is partly broken up into metaborate chains containing non-bridging oxygens. Thus, the intermediate range order within the B–O network is expected to be more complicated and less characteristic for the metaborate composition than for the tetra- and diborate glasses. This is confirmed by the present RMC modelling of $(AgI)_{0.6}$–$(Ag_2O$–$B_2O_3)_{0.4}$, which in figure 3(c) shows that none of the partial structure factors give evidence of any characteristic intermediate range distance in the glass. The result may seem to be in contradiction to the very intense FSDP at about 0.46 $Å^{-1}$ in the total $S(Q)$, but in the RMC model this peak is not due to any particular peak in the individual $S_{ij}(Q)$. Rather, the FSDP in the total $S(Q)$ is produced by the sum of partials with steadily increasing and decreasing intensities, respectively, for decreasing Q (in the actual Q-range). The partials with the most increasing intensities (with decreasing Q) are the three of the B–O network. This indicates that the density fluctuations (the degree of cluster–void tendency) are largest within the B–O network, but that no typical void size is present in the structure. Thus, the characteristic distance between neighbouring borate segments separated by voids in the network structure, which is present, to some extent, in the AgI doped tetraborate glasses and clearly in the highly AgI doped diborate glasses [17], seems to be almost lost in the metaborate glass. The network structure is more disordered and the distribution of void sizes more similar to what has been observed for the LiCl and NaCl doped diborate glasses [32]. This is, in fact, evident directly from a visual inspection of the model configuration. Figures 4(a) and (b) show a 10 Å thick slice of the RMC produced structure of the B–O network and the distributions of Ag^+ and I^- ions for the $(AgI)_{0.6}$–$(Ag_2O$–$B_2O_3)_{0.4}$ glass. In [17] corresponding pictures were shown for the $(AgI)_{0.6}$–$(Ag_2O$–$2B_2O_3)_{0.4}$ glass, and it was there clear that the voids in the B–O network are of relatively well-defined size (8 ± 3 Å) corresponding to the Q-value Q_1 of the FSDP ($2\pi/Q_1 \sim 8$ Å). Similar void sizes can also be observed in figure 4(a), but generally the voids

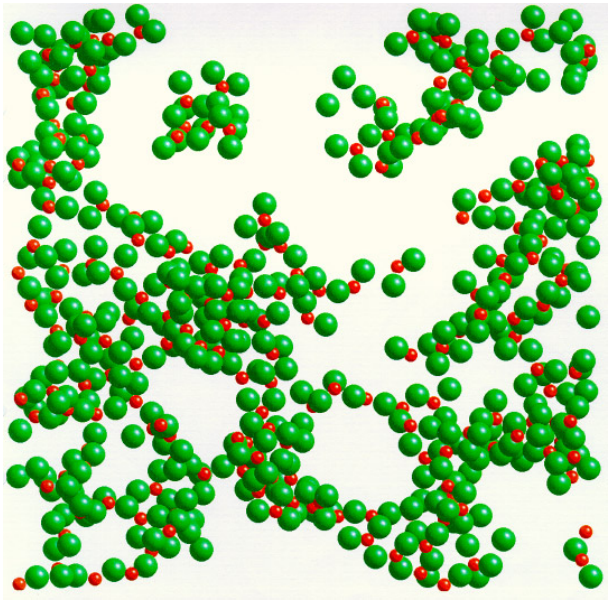

(a)

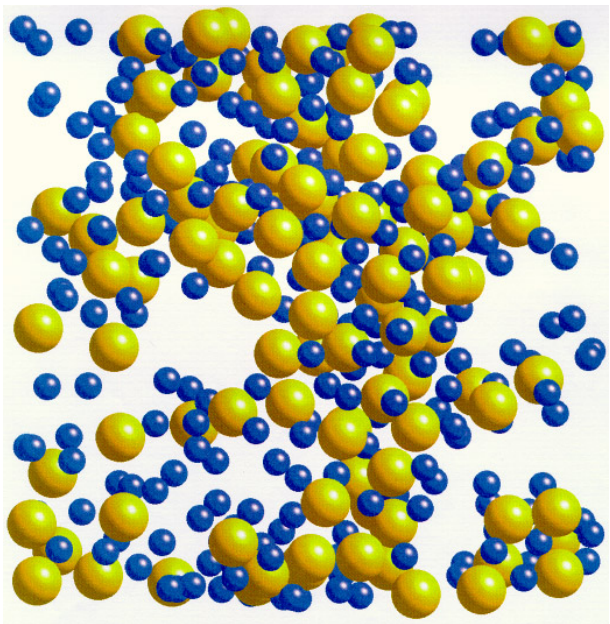

(b)

Figure 4. A 10 Å thick slice of a part of the RMC produced configuration of $(AgI)_{0.6}$–$(Ag_2O$–$B_2O_3)_{0.4}$: (a) shows the structure of the B–O network and (b) the distribution of silver and iodine ions. The radii of the chemical components are B = 0.5, O = 0.9, $Ag^+ = 1.0$ and $I^- = 1.8$ Å.

are larger with less defined size, which explains the high low Q intensity (without showing any clear peak) in $S_{BB}(Q)$, $S_{BO}(Q)$ and $S_{OO}(Q)$ of $(AgI)_{0.6}$–$(Ag_2O$–$B_2O_3)_{0.4}$. However, in order to make a definite statement of the seemingly less pronounced intermediate range order

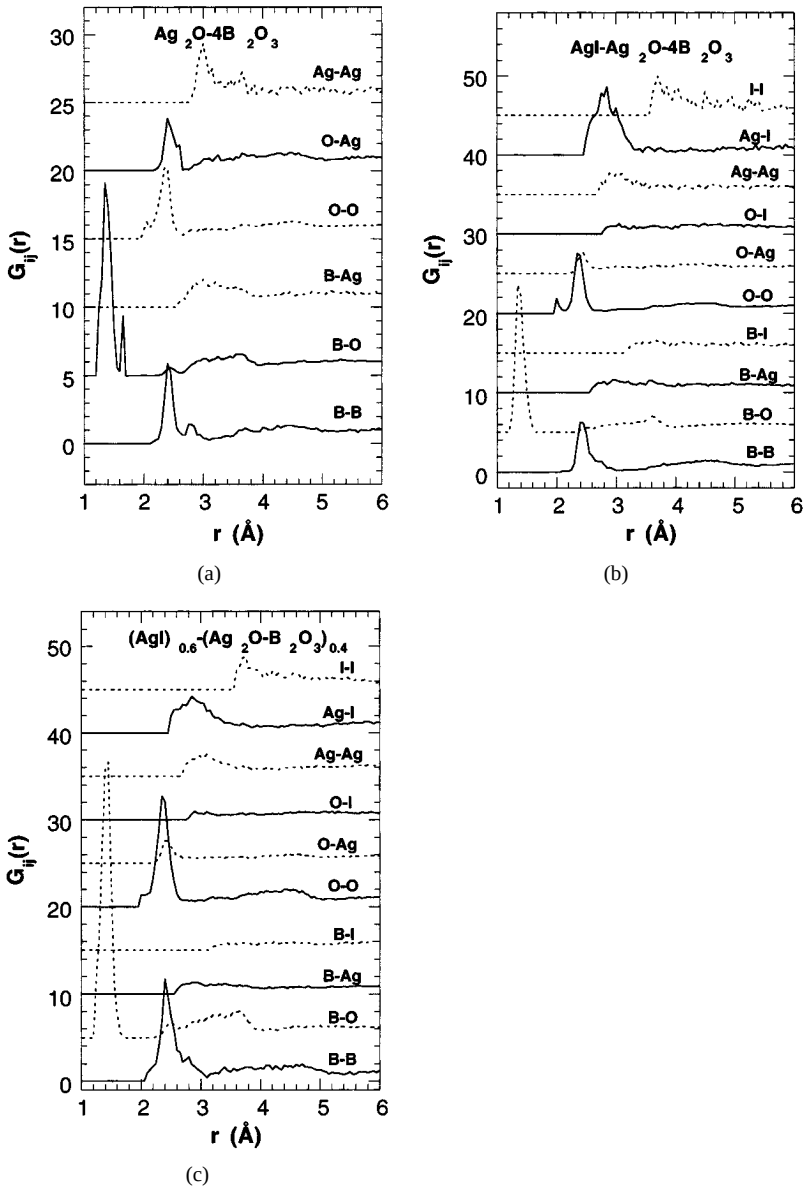

Figure 5. Partial pair correlation functions, $G_{ij}(r)$, obtained from the RMC produced configurations of (a) Ag_2O–$4B_2O_3$, (b) AgI–Ag_2O–$4B_2O_3$ and (c) $(AgI)_{0.6}$–$(Ag_2O$–$B_2O_3)_{0.4}$. Consecutive curves are shifted vertically by 5.0, for clarity.

within the B–O network of the metaborate glass one would need contrasting experimental x-ray diffraction data in the corresponding low Q-range 0.1–3 $Å^{-1}$.

From figure 4(a) it is also evident that the B–O network of $(AgI)_{0.6}$–$(Ag_2O$–$B_2O_3)_{0.4}$ shows 'clusters' of rather different sizes, in contrast to the corresponding diborate glass where the network is formed into a more ordered chainlike structure of diborate units [17]. Since the B–O network is 'clustered' and the silver and iodine ions are present in the voids between these 'clusters' it is obvious that also the salt ions have to be 'clustered' to some extent,

Table 1. Interatomic distances and average coordination numbers, N_{ij}, obtained from the RMC produced configurations of Ag_2O–$4B_2O_3$, AgI–Ag_2O–$4B_2O_3$ and $(AgI)_{0.6}$–$(Ag_2O$–$B_2O_3)_{0.4}$. In the calculations of N_{ij} the integrations were performed over the first peak in the corresponding $G_{ij}(r)$, i.e. up to the r-values 1.7 Å for B–O, 2.8 Å for Ag–O, 3.0 Å for B–B and O–O, 3.4 Å for Ag–I and 3.5 Å for Ag–Ag. The error bars have been estimated from the differences observed between several configurations of the present glasses. The average coordination numbers for B–O are determined directly from the experimental $G(r)$. The NMR based B–O coordination number [23] constraints applied in the RMC modelling are given in brackets.

	Glass composition					
	Ag_2O–$4B_2O_3$		AgI–Ag_2O–$4B_2O_3$		$(AgI)_{0.6}$–$(Ag_2O$–$B_2O_3)_{0.4}$	
Atomic pair	Distance	N_{ij}	Distance	N_{ij}	Distance	N_{ij}
B–B	2.42 ± 0.02	3.3 ± 0.3	2.42 ± 0.02	3.3 ± 0.3	2.40 ± 0.02	3.0 ± 0.3
B–O	1.37 ± 0.01	3.14 [3.25]	1.37 ± 0.01	3.21 [3.25]	1.43 ± 0.01	3.45 [3.53]
O–O	2.37 ± 0.02	5.5 ± 0.5	2.37 ± 0.02	5.2 ± 0.5	2.37 ± 0.02	5.5 ± 0.5
Ag–O	2.41 ± 0.1	3.3 ± 0.5	2.45 ± 0.1	1.9 ± 0.4	2.44 ± 0.1	1.0 ± 0.3
Ag–Ag	3.0 ± 0.2	1.0 ± 0.3	3.05 ± 0.1	1.7 ± 0.4	3.05 ± 0.1	3.3 ± 0.5
Ag–I			2.85 ± 0.1	1.2 ± 0.3	2.85 ± 0.1	2.2 ± 0.4

i.e. they cannot occupy space which is occupied by the B and O atoms. This is clearly seen in figure 3(c), which shows that the intensities of $S_{AgAg}(Q)$, $S_{AgI}(Q)$ and $S_{II}(Q)$ increase (however less rapidly than for $S_{BB}(Q)$, $S_{BO}(Q)$ and $S_{OO}(Q)$) with decreasing Q in the low Q-range. From figure 4(b) there is, however, no doubt about that the salt ions are much less 'clustered' and, thus, more homogeneously distributed than the B and O atoms. As for the AgI doped tetra- and diborate glasses the four partials involving correlations between the salt ions and the network atoms are very flat, indicating that these correlations are weak and that the salt ions do not participate in the network formation.

4.3.2. Short range order. Figures 5(a)–(c) show the partial pair correlation functions $G_{ij}(r)$ for Ag_2O–$4B_2O_3$, AgI–Ag_2O–$4B_2O_3$ and $(AgI)_{0.6}$–$(Ag_2O$–$B_2O_3)_{0.4}$, respectively. By comparing the three figures it is clear that the short range order within the B–O network is similar for the three glasses. This is further evident from the summary of interatomic distances and coordination numbers N_{ij}, which were obtained from the positions and integrated areas of the first peak in the partial $G_{ij}(r)$, given in table 1. As for the experimental total $G(r)$ the most significant difference is the substantially larger first B–O distance (1.43 Å) in $(AgI)_{0.6}$–$(Ag_2O$–$B_2O_3)_{0.4}$ compared to the two tetraborate glasses (1.37 Å), indicating that a larger fraction of the borons in the metaborate glass has a longer B–O distance typical of four-coordinated borons [16]. The interatomic distances involving Ag^+ ions are also similar for the three glasses, as seen in table 1. The nearest neighbour correlations, Ag–B, I–B and I–O show only broad peaks (see figures 5(a)–(c)), indicating that particularly the I^- ions are very weakly connected to the boron–oxygen network. However, in the case of the broad peak of Ag–B one should note that also the crystalline phase of Ag_2O–$4B_2O_3$ contains many different Ag–O, Ag–B and Ag–Ag distances [33]. Thus, the Ag^+ ions are asymmetrically coordinated in the crystalline phase, so the pair distance distributions involving Ag are expected to be rather broad in the glasses, even for well defined Ag sites. The distribution of Ag^+ ions is, however, clearly different in the RMC model of glassy Ag_2O–$4B_2O_3$ than in the corresponding crystalline phase, where the shortest Ag–Ag distance is as long as 3.69 Å.

From the distributions of Ag–O and Ag–I coordination numbers given in figures 6(a)–(c) and the average coordination numbers given in table 1 it is clear that the Ag–O coordination

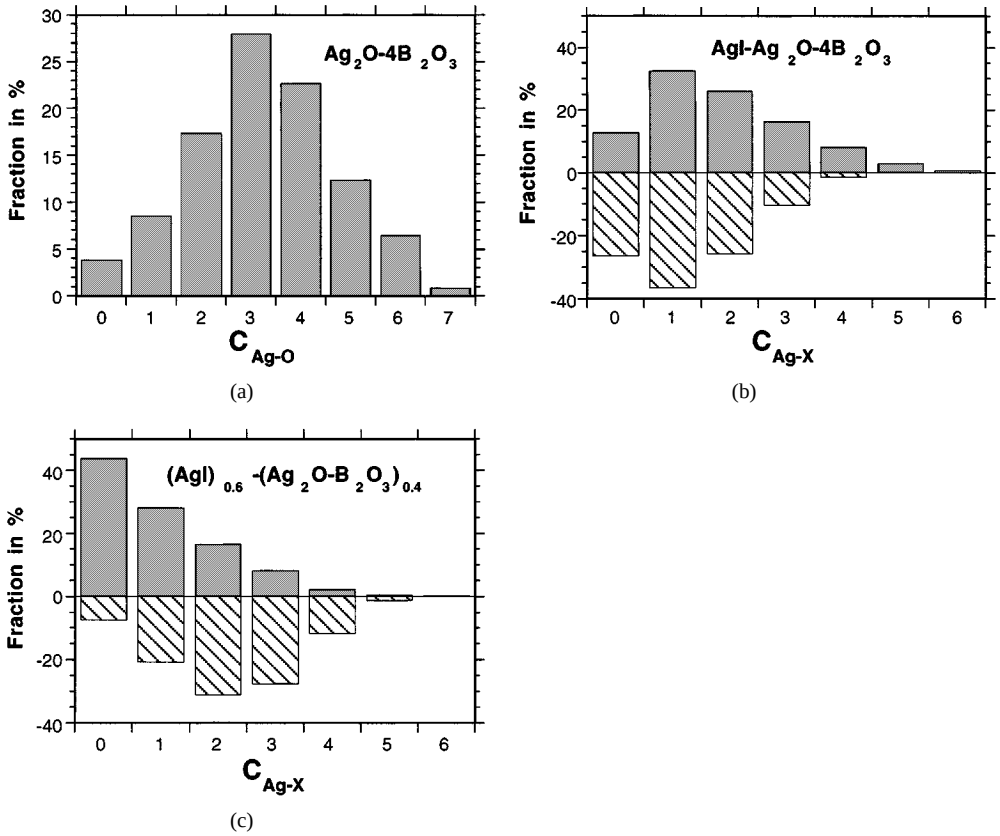

Figure 6. Distributions of Ag–O (positive bars) and Ag–I (negative bars) coordination numbers calculated from the RMC produced configurations of (a) Ag_2O–$4B_2O_3$, (b) AgI–Ag_2O–$4B_2O_3$ and (c) $(AgI)_{0.6}$–$(Ag_2O$–$B_2O_3)_{0.4}$.

is almost identical for Ag_2O–$4B_2O_3$ to that previously observed for Ag_2O–$2B_2O_3$ [17]. When AgI is introduced the Ag^+ ions partly dissociate from the oxygens and for the AgI–Ag_2O–$4B_2O_3$ composition the majority of the silver ions are coordinated to both O and I^-. This dissociation effect increases with increasing dopant concentration for the tetra-, di- and metaborate glasses. However, for a certain dopant concentration the dissociation seems to be approximately the same for the tetra- and diborate compositions, whereas the effect is considerably stronger for the metaborate composition. For the $(AgI)_{0.6}$–$(Ag_2O$–$B_2O_3)_{0.4}$ glass more than 40% of the Ag^+ ions reside in an iodine environment (see figure 6 and table 1), which is a much higher fraction than in other similarly doped network glasses, such as $(AgI)_{0.6}$–$(Ag_2O$–$2B_2O_3)_{0.4}$ and AgI–$AgPO_3$ [8]. The ratio of silver ions coordinated to I^- and O (i.e. the N_{AgI}/N_{AgO} ratio) is, in fact, as high as for the much higher doped $(AgI)_{0.75}$–$(Ag_2MoO_4)_{0.25}$ glass [8], which has about three times as high conductivity as the metaborate glass [2, 6]. This result, in combination with the large voids in the B–O structure (see figure 4(a)), indicates that the highly doped metaborate glasses contain some smaller clusters of AgI (∼10 Å) which are likely to crystallize if they grow substantially more. Finally, one should note from table 1 that although the nearest Ag–Ag distance is the same (about 3 Å) for the three glasses, the average Ag–Ag coordination number increases substantially with increasing Ag concentration.

5. Discussion

The structures of the glasses studied here show several analogies to the previously studied AgI doped diborate glasses [17], but also some clear differences. The most striking difference is probably the rather different intermediate range order of the AgI doped tetra-, di- and metaborate glasses. The diborate $(AgI)_{0.6}$–$(Ag_2O$–$2B_2O_3)_{0.4}$ showed a substantially ordered intermediate range structure with just one clearly observed characteristic distance of 8 ± 3 Å within the B–O network [17]. For the low network modified tetraborate AgI–Ag_2O–$4B_2O_3$ glass there are relatively large (or many) regions present with no salt ions, where the characteristic intermediate range distance is close to the value for pure B_2O_3, i.e. about 4 Å [30], whereas the intermediate range order of the salt rich regions is similar to that of the AgI doped diborate glass and shows a characteristic distance of about 8 Å. Similar differences and similarities are also observed between the undoped tetra- and diborate glasses. For the AgI doped metaborate glass the voids within the B–O network are generally larger, but also of less defined size and less correlated, which gives no clearly pronounced intermediate range characteristic distance. Thus, the network structures of both the tetra- and metaborate glasses seem to be slightly more disordered than for the previously studied diborate glass [17]. All the short range order distances (for all the partial correlations) are however similar for the studied (including the diborates [17]) undoped and AgI doped glasses (see table 1).

5.1. Structural implications on ion conduction

Let us now discuss the implications of the structural results on the ionic conductivity. It has already been mentioned that the large differences in ionic conductivity between the undoped and low AgI doped tetra-, di- and metaborate glasses (up to five orders of magnitude [6]) have almost vanished at high dopant concentrations, and there seems to exist a 'saturation effect' of the conductivity for highly conducting glasses. This can, in fact, be understood from the present structural findings as will be discussed in this section. Let us begin by comparing the tetra- and diborate glass systems $(AgI)_x$–$(Ag_2O$–$4B_2O_3)_{1-x}$ and $(AgI)_x$–$(Ag_2O$–$2B_2O_3)_{1-x}$. The conductivities of the undoped tetra- and diborate glasses are approximately 10^{-11} and 10^{-7} S cm^{-1}, and for the $x = 0.6$ doped glasses the corresponding values have increased to about 3×10^{-4} and 10^{-3} S cm^{-1}, respectively [6]. Since the local environments of the Ag^+ ions are the same for the undoped tetra- and diborate glasses, except for the higher Ag–Ag coordination number for the diborate glass, the difference between their conductivities is likely to be explained by a larger number of available and energetically favourable Ag sites in the diborate glass. The average Ag–Ag coordination number increases from about 1.0 for the undoped tetraborate composition to approximately 2.0 [17] for the diborate glass. This means that there should be a substantially more extended network of migration pathways in the diborate glass (where 2 is the lowest possible Ag–Ag coordination number for an Ag^+ ion participating in such a pathway network). When a large amount of AgI is introduced the average Ag–Ag coordination number increases to about 1.7 for AgI–Ag_2O–$4B_2O_3$, whereas it remains the same (about 2.0 [17]) for the $x = 0.6$ doped diborate glass. This may explain the reduced difference in conductivity between the highly doped tetra- and diborate glasses, since the Ag^+ ions have similar local environments (i.e. similar nearest Ag–O, Ag–I and Ag–Ag distances and coordination numbers) in the two glasses. Furthermore, for both glasses there is a separation of about 8 Å between B–O segments separated by 'Ag pathways'. Thus, both the short and intermediate range structural results show strong evidence that the Ag^+ ions have similar local environments and conduction pathways in the highly doped tetra- and diborate glasses. It should also be noted that the induced salt ions simultaneously expand

the B–O network and contribute to a partial dissociation of the Ag^+ ions from oxygens. This is likely to cause new and more energetically favourable pathways for the silver ions and thus explain the rapid increase in conductivity with increasing salt concentration for both glasses.

For most AgI doped oxide glasses the ionic conductivity seems to be closely related to the expansion of the glass matrix as well as the degree of dissociation of the Ag^+ ions from the oxygens [7, 8]. However, the highly AgI doped metaborate glasses differ slightly from these relations, which predict that the conductivity of the $(AgI)_{0.6}$–$(Ag_2O–B_2O_3)_{0.4}$ glass should be a factor of approximately three higher (1.2×10^{-2} S cm^{-1} rather than the observed 4×10^{-3} S cm^{-1} [6]). From the present structural results there are two possible explanations for the reduced conductivity. First, the metaborate glass shows evidence of small (∼10 Å) clusters of AgI, which were not observed in the RMC produced models of AgI doped diborate [8, 17], metaphosphate [8, 34], tungstate [35] and molybdate [8, 35] glasses, and second, the metaborate glass has a significantly higher average Ag–Ag coordination number (about 3.3) than was observed for the other above given AgI doped oxide glasses, where the Ag–Ag coordination numbers were around 2. Recent investigations have indicated that both these structural features may be detrimental for the conductivity [9, 29, 36]. Investigations based on the bond valence pseudopotential method [29] and molecular dynamics (MD) simulations [36], of the most energetically favourable migration pathways in AgI doped crystalline [29] and glassy [36] ionic conductors indicated that the silver ions prefer to jump between sites of similar local environments. This implied that the Ag^+ ions which were coordinated to only I^- ions were highly mobile only within these restricted regions, and consequently they did not make any strong contribution to the total conductivity [29, 36]. Instead, the conductivity was mainly determined by the Ag^+ ions with a mixed iodine and oxygen coordination, which formed the most extended network of connected energetically favourable Ag sites [29, 36]. Thus, the present observation of small clusters of AgI in the $(AgI)_{0.6}$–$(Ag_2O–B_2O_3)_{0.4}$ glass may, in fact, be detrimental for the conductivity (or at least not make any significant contribution) provided that the clusters are not connected to macroscopically percolating pathways, since the presence of such clusters reduces the number of Ag^+ ions with a mixed iodine–oxygen environment.

The other explanation for the reduced conductivity as well as the non-Arrhenius behaviour observed for highly conducting crystalline and glassy electrolytes [1, 3–5] is the extraordinary high Ag–Ag coordination number, which according to Maass *et al* [9] should cause a decrease of the conductivity due to Coulomb interactions between the mobile Ag^+ ions. If this is the case there should be an intermediate Ag–Ag coordination number (probably of about 2) which is optimal for the conductivity. If the coordination number is too low there will be too few energetically favourable cationic sites around each Ag^+ ion to form a macroscopic network of migration pathways and the conductivity will consequently be reduced due to the necessity of using paths with considerably higher activation energies for ionic diffusion. If, on the other hand, the coordination number is too high, the Coulombic term of the activation energy will increase, particularly at high temperatures [9], and the conductivity reaches a 'saturation effect' manifested as a non-Arrhenius behaviour at high enough temperature.

6. Conclusion

The present neutron diffraction and RMC study of the ion conducting glasses $Ag_2O–4B_2O_3$, $AgI–Ag_2O–4B_2O_3$ and $(AgI)_{0.6}$–$(Ag_2O–B_2O_3)_{0.4}$ shows that the most significant difference between the glasses is the higher fraction of four coordinated borons in the metaborate glass. Also on an intermediate range length scale there are large differences between the investigated glasses. The structure of $Ag_2O–4B_2O_3$ can be described as a mixture of two micro regions

with structures similar to $Ag_2O–2B_2O_3$ and pure B_2O_3. Two characteristic intermediate range distances are then observed: one between neighbouring B–O segments separated by bridging Ag^+ ions and one where voids separate the B–O segments. For the AgI doped tetraborate glass the situation is similar and its structure can be regarded as a mixture of $AgI–Ag_2O–2B_2O_3$ and pure B_2O_3, where the longest characteristic distance of about 8 Å is a typical distance between B–O segments separated by Ag–I–Ag bridges (simplified picture). The intermediate range order of the $(AgI)_{0.6}–(Ag_2O–B_2O_3)_{0.4}$ glass is rather different from the correspondingly doped tetra- and diborate glasses due to a generally more disordered structure with voids of widely different sizes within the B–O network and the presence of small (∼10 Å) clusters of AgI.

The findings for the metaborate glass of an extraordinary high Ag–Ag coordination number and a comparably small number of Ag^+ ions with a mixed oxygen–iodine environment may be detrimental for the ionic conductivity and explain why the highly AgI doped metaborate glasses have slightly lower conductivities than is predicted from the salt induced expansion of the glass forming network and the local average environment of the Ag^+ ions. The high Ag–Ag coordination may, furthermore, give rise to a strong cationic Coulomb interaction, which has been proposed [9] to increase the activation energy for ionic diffusion and result in a non-Arrhenius temperature behaviour of the conductivity.

Acknowledgment

This work was financially supported by the Swedish Natural Science Research Council.

References

[1] Kincs J and Martin S W 1996 *Phys. Rev. Lett.* **76** 70
[2] Kawamura J and Shimoji M 1989 *Mater. Chem. Phys.* **23** 99
[3] Liu C and Angell C A 1986 *J. Non-Cryst. Solids* **83** 162
[4] Saito T, Torata N, Tatsumisago M and Minami T 1996 *Solid State Ion.* **86–88** 491
[5] Ribes M, Taillades G and Pradel A 1998 *Solid State Ion.* **105** 159
[6] Schiraldi A and Pezzati E 1989 *Mater. Chem. Phys.* **23** 75
[7] Swenson J and Börjesson L 1996 *Phys. Rev. Lett.* **77** 3569
[8] Swenson J, McGreevy R L, Börjesson L and Wicks J D 1998 *Solid State Ion.* **105** 55
[9] Maass P, Meyer M, Bunde A and Dieterich W 1996 *Phys. Rev. Lett.* **77** 1528
[10] Ngai K L and Rizos A K 1996 *Phys. Rev. Lett.* **76** 1296
[11] Börjesson L 1987 *Phys. Rev.* B **36** 4600
[12] Börjesson L and Torell L M 1987 *Solid State Ion.* **25** 85
[13] Howells W S 1980 *Rutherford–Appleton Laboratory Report* RAL-80-017
Howells W S 1986 *Rutherford–Appleton Laboratory Report* RAL-86-042
[14] Howe M, Howells W S and McGreevy R L 1989 *J. Phys.: Condens. Matter* **1** 3433
[15] Lorch E 1969 *J. Phys. C: Solid State Phys.* **2** 229
[16] Swenson J, Börjesson L and Howells W S 1995 *Phys. Rev.* B **52** 9310
[17] Swenson J, Börjesson L, McGreevy R L and Howells W S 1997 *Phys. Rev.* B **55** 11 236
[18] McGreevy R L and Pusztai L 1988 *Mol. Simul.* **1** 359
[19] Keen D A and McGreevy R L 1990 *Nature* **344** 423
[20] McGreevy R L 1992 *Annu. Rev. Mater. Sci.* **22** 217
[21] McGreevy R L 1995 *Nucl. Instrum. Methods Phys. Res.* A **354** 1
[22] Metropolis N, Rosenbluth A W, Rosenbluth M N, Teller A H and Teller E 1953 *J. Phys. Chem.* **21** 1087
[23] Chiodelli C, Magistris A, Villa M and Bjorkstam J L 1982 *J. Non-Cryst. Solids* **51** 143
[24] Feller S A, Dell W J and Bray P J 1982 *J. Non-Cryst. Solids* **51** 21
[25] Galeener F, Lucovsky G and Mikkelsen J C Jr 1980 *Phys. Rev.* B **8** 3983
[26] Lorösch J, Couzi M, Pelous J, Vacher R and Levasseur A 1984 *J. Non-Cryst. Solids* **69** 1
[27] Kamitsos E I, Patsis A P, Karakassides M A and Chryssikos G D 1990 *J. Non-Cryst. Solids* **126** 52

[28] Radaev S F, Fink L, Trömel M 1994 *Z. Kristallogr. Suppl.* **8** 628
Trömel M 1997 Private communication
[29] Adams S and Maier J 1998 *Solid State Ion.* **105** 67
[30] Swenson J and Börjesson L 1998 *J. Non-Cryst Solids* **223** 223
[31] Cervinka L, Bergerova J, Dalmaso A and Rocca F 1998 *J. Non-Cryst. Solids* **232–234** 627
[32] Swenson J, Börjesson L and Howells W S 1998 *Phys. Rev.* B **57** 13 514
[33] Krogh-Moe J 1965 *Acta Crystallogr.* **18** 77
[34] Wicks J, Börjesson L, McGreevy R L, Howells W S and Bushnell-Wye G 1995 *Phys. Rev. Lett.* **74** 726
[35] Swenson J, McGreevy R L, Börjesson L, Wicks J D and Howells W S 1996 *J. Phys.: Condens. Matter* **8** 3545
[36] Karthikeyan A and Rao K J 1997 *J. Phys. Chem.* B **101** 3105